American Journal of Pathology, Vol. 155, No. 1, July 1999

Lipid Deposition in Rat Aortas with Intraluminal Hemispherical Plug Stenosis

A Morphological and Biophysical Study

Thomas Zand,* Allen H. Hoffman,† Brian J. Savilonis,† Jean M. Underwood,* John J. Nunnari,* Guido Majno,* and Isabelle Joris*

From the Department of Pathology, University of Massachusetts Medical School, Worcester, Massachusetts; and the Department of Mechanical Engineering,† Worcester Polytechnic Institute, Worcester, Massachusetts*

A new method was devised to create a stenosis in the rat abdominal aorta. To restrict blood flow, a hemispherical plug was inserted into the aorta through a renal artery. This type of intrinsic (intraluminal) stenosis minimizes possible intramural effects associated with external compression or ligation which severely deform the arterial wall. In the aorta of hypercholesterolemic rats, lipid deposits were distributed in crescent-shaped patches proximal and distal to the plug, whereas lipid deposition in the opposite aortic wall was inhibited. Based on enlarged physical scale models used to study the flow field, the regions of lipid deposition were found to coincide with regions of low shear stress, stagnation, and recirculation. Shear stress was elevated at the wall opposite the plug. These results show that when confounding mural effects are minimized, lipid deposition is promoted in regions of low shear stress with recirculation and inhibited in regions of elevated shear stress. ***(Am J Pathol 1999, 155:85–92)***

The genesis and location of atherosclerotic plaques have been related to various hydrodynamic factors such as flow disturbances, shear stress, turbulence, boundary layer separation, and fluctuations in shear stress.[1–3] The role of these factors has been investigated in animal models,[4–14] *in vitro* models,[15–24] physical scale models,[13,14,25] and mathematical-computational simulated models.[26] Typically, in the *in vivo* studies, flow and lipid deposition were studied in arteries narrowed by a ligature[5–7,10–12] or by a metal clip[13,14] applied externally. Such models are subject to criticism because, in addition to causing flow disturbances, an extrinsic stenosis creates intramural stresses and strains, which may have an impact on lipid deposition in the intima.[14,27] Compressing the arterial wall from the outside can only partially simulate the narrowing of the artery that occurs spontaneously *in vivo*. We therefore designed a new experimental model of stenosis of the rat aorta that avoids compression of the aortic wall, thereby minimizing the effect on intramural stresses. The aorta is restricted from the inside by inserting a small, mushroom-shaped Plexiglas plug into the aortic lumen through the ostium of a severed renal artery. At its apex, the intraluminal plug reduced the cross-sectional area of the lumen by approximately 50%. The rats were then made hypercholesterolemic, and the topography of the lipid deposits in relation to the plug stenosis was studied morphologically.

Materials and Methods

Animals

Twelve male Wistar rats (Charles River Breeding Laboratories, Wilmington, MA) 4–6 weeks of age and weighing 225–250 g were maintained in accordance with the recommendations in the *Guide for the Care and Use of Laboratory Animals* (DHHS, NIH Publication No. 85–23, 1985) and guidelines of the Animal Care Advisory Committee of the University of Massachusetts Medical School.

Stenosis

Mushroom-shaped Plexiglas plugs were prepared by the University of Massachusetts Medical School machine shop using a 10-inch Hardinge lathe. The nearly hemispherical cap measured approximately 0.9 × 1.5 mm and the stem 3 × 1 mm (Figure 1). These dimensions were chosen within the limits imposed by the size of the

Supported in part by grants HL25973 and HL33529 from the National Heart, Lung and Blood Institute. Contents are solely the responsibility of the authors and do not necessarily represent the official views of the National Institutes of Health.

Accepted for publication April 15, 1999.

Address reprint requests to Isabelle Joris, Ph.D., Department of Pathology, University of Massachusetts Medical School, 55 Lake Avenue North, Worcester, Massachusetts 01655-0125.

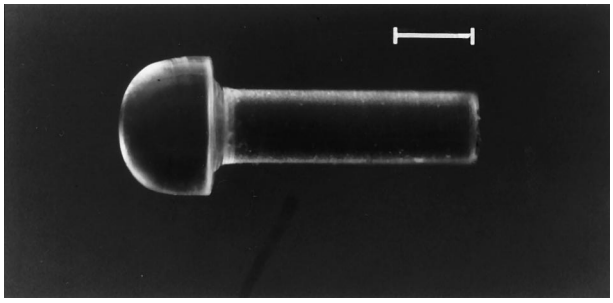

Figure 1. Hemispherical Plexiglas plug. Scale bar, 1 mm.

aortic system in the rat for the purpose of creating an approximately 50% occlusion of the aortic lumen.

Surgery

Under Nembutal anesthesia administered intraperitoneally, the rat was laid supine and a 5-cm incision was made along the linea alba. The left renal artery and vein were cleared of overlying peritoneum and fat, and the aorta was isolated 5 mm proximal and distal to the left renal vessels. The left renal artery was ligated with 4–0 silk 4–5 mm from its aortic origin. The left renal vein was double-ligated 2 mm from its entrance into the inferior vena cava and sectioned between ligatures. The abdominal aorta was then cross-clamped with atraumatic aneurysm clips 1 mm below the right renal artery and 5 mm below the left renal artery. When needed, an additional clamp was placed across adjacent spermatic branches. The left renal artery was sectioned 2–3 mm from the aorta, dilated and held open with no. 5 jeweler's forceps. The plug was inserted through the renal artery stump into the lumen of the aorta using a microneedle holder. This required gentle force because the head of the plug was wider than the natural lumen of the renal artery. Two 8–0 nylon ligatures were then placed around the renal artery,

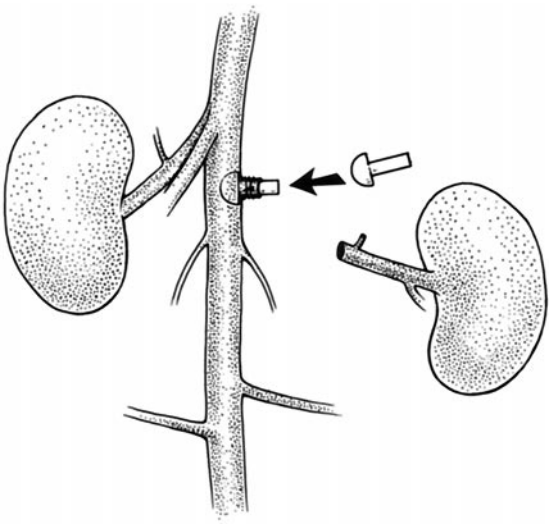

Figure 2. Insertion and positioning of a plug in the rat aorta. Diagram of the surgical procedure in which the plug is inserted through the severed left renal artery into the aortic lumen.

Figure 3. Excised and perfusion-fixed aorta seen by transillumination. The plug is seen in the severed left renal artery. At the apex of this plug the aortic lumen was narrowed by about 50%. The plug was in place for 4 months and the rat was hypercholesterolemic for 3 months. Original magnification, ~10×.

which cuffed the stem of the plug. The aortic clamps were then removed, the left kidney and adrenal gland were excised, and minor bleeding vessels were cauterized. The abdominal wall was closed with 4–0 silk running sutures; the skin was closed with stainless steel clips. The entire surgical procedure (Figure 2) lasted approximately 30 minutes, after which the animal was returned to its cage and fed a normal diet.

Experimental Design

Twelve rats were used. Stenosis was produced in six; six were kept as unstenosed controls. The rats with stenosis were fed a normal diet for 1 month to allow recovery and healing from surgery; thereafter, they were placed on a hypercholesterolemic diet for 3 months. The controls were also fed a hypercholesterolemic diet for 3 months after 1 to 4 weeks on a normal diet.

The purpose of the experiment was to compare the pattern of lipid deposition in unstenosed rats with that in rats with the plug stenosis. Surgical sham controls were not performed; ligating the renal artery would have cre-

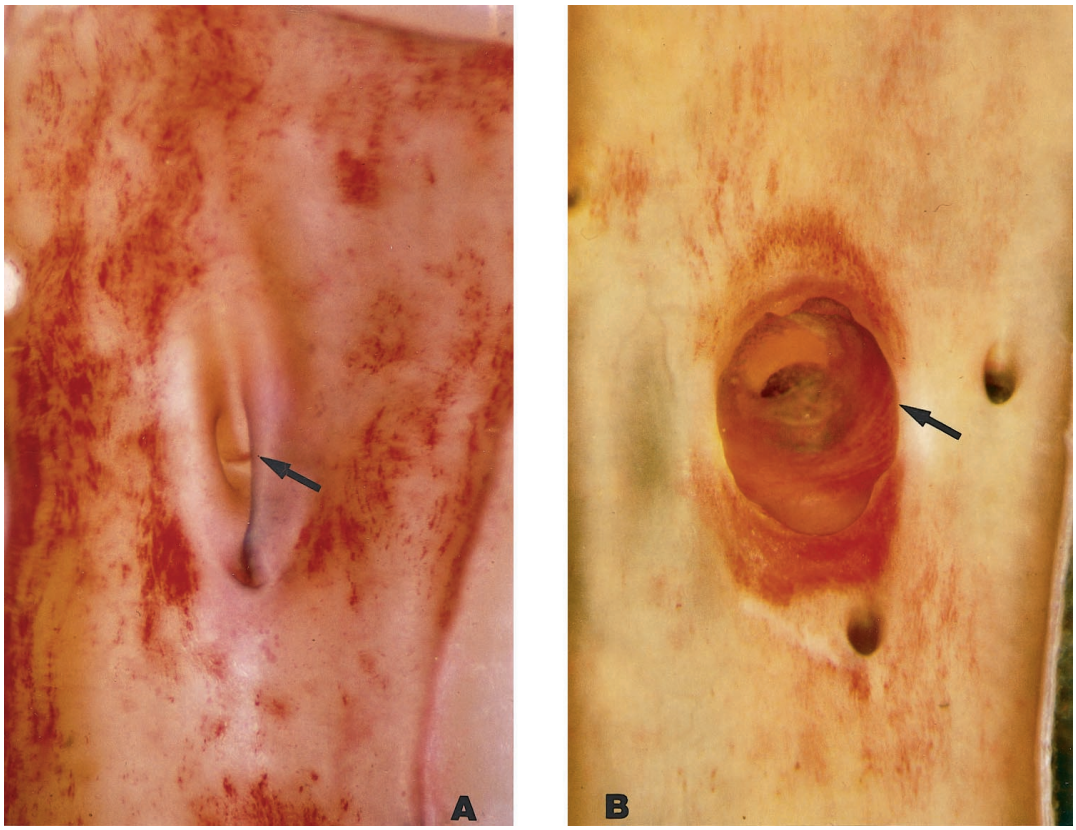

Figure 4. Rat abdominal aortas seen *en face* after 3 months of hypercholesterolemia. Blood flow is from top to bottom (Oil red O; original magnification, ~15×). A: Control (non-stenosed aorta): the left ostium is in the center (arrow). Patches of oil red O lipid are scattered at random in the intima. B: Stenosed aorta with plug in place for 4 months. The cap (arrow) of the plug is overgrown with neointima except for the clear area at top left. The dark disk in the center of the plug corresponds to the stem of the plug fitted in the renal artery ostium and viewed head-on through the cap of the plug. Heavily stained crescent-shaped lipid deposits are located upstream, downstream, and at the base of the plug. On average the proximal region extended upstream 0.5 diameters and the distal region extended downstream 1.5 diameters There is no lipid deposition on the left and right sides of the aorta, which correspond *in vivo* to the aortic surface opposite the apex of the plug.

ated a new geometry of the aorta not directly relevant to the experimental model.

Diets

Hypercholesterolemia was induced by feeding the rats *ad libitum* a diet supplemented with 4% cholesterol, 1% cholic acid, and 0.5% 2-thiouracil (CCT Diet, Bioserve, Frenchtown, NJ).[28] Normal diet was standard Purina Lab Chow No. 5008 (Ralston Purina, St. Louis, MO).

Plasma Cholesterol

Before sacrifice, 1 ml of blood was obtained for measuring plasma cholesterol using Sigma kit 351-20 (Sigma Chemical, St. Louis, MO).

Perfusion Fixation and Intimal Staining

Under deep ether anesthesia, the rats were sacrificed by perfusion-fixation at 110 mm Hg.[28] Perfusion staining of the intercellular junctions with silver nitrate and of lipid deposits with oil red O was performed as previously described.[14]

Light Microscopy

One-centimeter segments of the fixed and oil red O-stained abdominal aortas, containing the plug site in stenosed animals (Figure 3) and the corresponding aortic segment in controls, were cut open longitudinally along the right lateral wall, pinned flat on paraffin, immersed in water, and viewed *en face* through a surgical microscope. The plugged aorta of one hypercholesterolemic rat was set aside for embedding in Epon as previously described.[14] Semithin 1-μm longitudinal sections through the stenosis site were cut and stained with toluidine blue.

En Face *Mapping of Lipid Deposits*

The aortic segment containing the plug site was opened, pinned out, and photographed. A Kodachrome slide was projected onto paper and the perimeter of the aortic

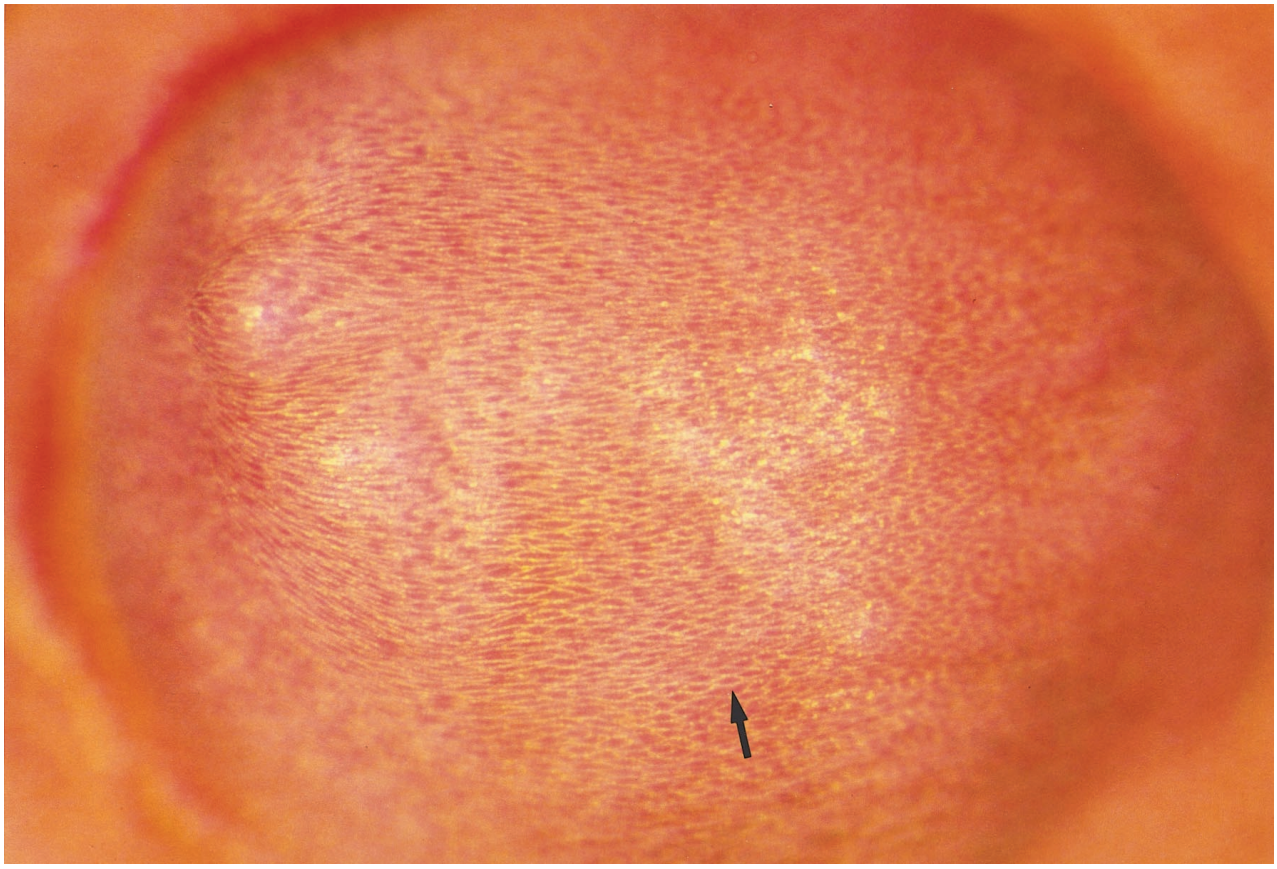

Figure 5. Surface of the plug seen *en face*. It is completely covered by a neointima. The outlines of endothelial cells are stained with silver and visible as a fine flagstone pattern. The cells (arrow) are oriented in the direction of flow, left to right. (Silver staining and oil red O; original magnification, 90×)

specimen and outlines of all fat deposits were traced. The same procedure was carried out with the controls.

Biophysical Models: Hydrodynamic Studies

Dye streamline analysis was used to study the flow field in an enlarged 34:1 scale Plexiglas model of the *in vivo* hemispherical plug stenosis. In the model, the radius of the aorta and hemispherical plug were equal (25.4 mm).

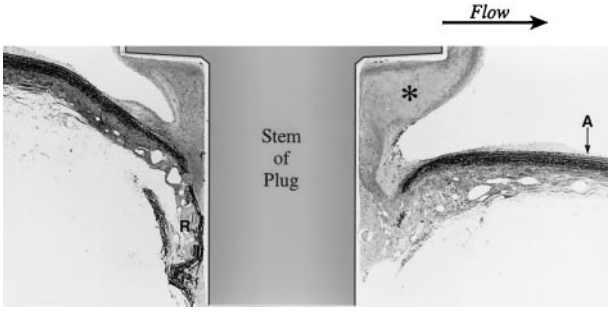

Figure 6. Stenosed aorta: longitudinal section of the aorta through the axis of the plug. Flow is from left to right. There is intimal thickening at the base of the plug and at the ostium between the aorta (A) and renal artery (R). Neointimal growth (*) along the distal edge of the plug is considerably greater than at the proximal edge. (One-micron Epon section, Toluidine blue; original magnification, ~40×)

To ensure fully developed flow, a straight entrance region 5 m long preceded the transparent test section.

In unsteady flow, the Strouhal number[29] is a dimensionless quantity that compares the relative importance of the local time-varying component of acceleration due to pulsatile flow to the convective component of acceleration due to changes in vessel geometry. A small Strouhal number indicates that the acceleration terms caused by changes in vessel geometry predominate. Based on the low Strouhal number (0.04) found in rats,[13] the flow in the region of the stenosis may be considered quasi-steady.

Hence, in a first study, a steady flow with mean (systolic) Reynolds number of 250 was analyzed. Water was maintained at a constant flow rate in the 5.1-cm diameter Plexiglas tube. Dye was injected at 40 different locations and the pathlines were recorded by videotaping at a frame rate of 60 frames/second. Mirrors allowed the simultaneous viewing of the velocity components in both the frontal and sagittal planes. A total of 1100 velocities were measured and *en face* wall shear stresses computed from the resulting velocity profiles. The wall shear stresses measured along the center line of the plug were normalized using the wall shear stress τ_o found in an unobstructed vessel with the same flow rate. This quantity, τ/τ_o, was then plotted as a function of axial position.

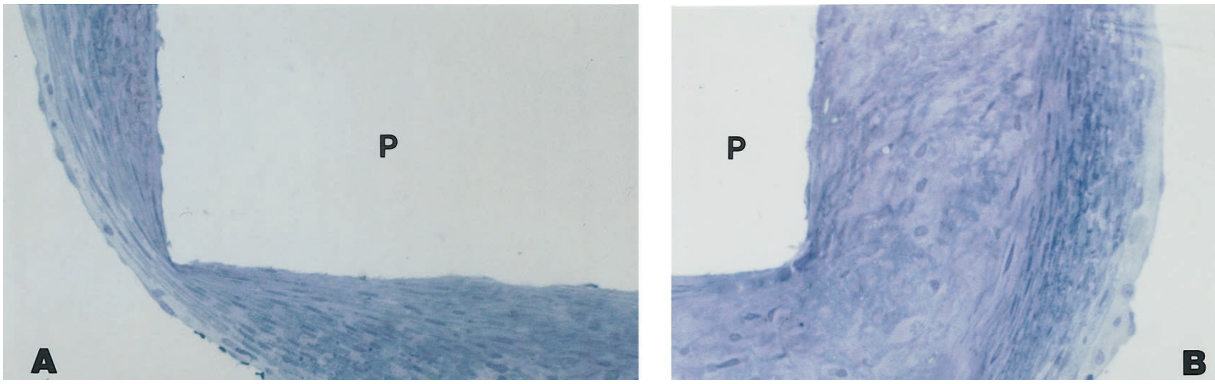

Figure 7. Neointima covering the base of the plug (P) consists of the endothelial lining over a layer of smooth muscle cells with some elastin. (P) represents the space left by the plug. Flow is from left to right. (One-micron Epon section, Toluidine blue; original magnification, 270×). A: Proximal edge. B: Distal edge.

In a second study, a sinusoidal flow pulse equal to 20% of the total flow was created using a rotating ball valve and superimposed on the steady flow component. The fluid was a 65% glycerol/35% water mixture. The mean Reynolds number was 250 and the Strouhal number was 0.04 (Womersley number of 1.6).[13,29] As with the steady flow experiments, dye visualization studies were used to determine the time-dependent extent of the low-velocity/recirculating regions near the plug.

Results

Animal Model

Hypercholesterolemic Controls without Plug Stenosis

Plasma cholesterol at time of sacrifice was greater than 500 mg/dl. The aortic intima viewed *en face* showed extensive, spotty, disseminated lipid deposits; their distribution appeared to be random except for some selectivity for arterial ostia, especially that of the left renal artery (Figure 4A).

Plug Stenosis with Hypercholesterolemia

Plasma cholesterol at time of sacrifice was greater than 500 mg/dl. A narrow band of oil red O-positive lipid was seen all around the base of the plug; heavier, crescent-shaped deposits were present proximally and distally. On average, the oil red O-positive proximal region extended upstream 0.5 diameters and the distal region extended downstream 1.5 diameters. The aortic intima opposite the plug contained almost no lipid. The surface of the plug had little or no lipid near the apex and small droplets were scattered over the rest of the hemisphere. As in the control arteries from hypercholesterolemic rats, lipid deposits were also seen at the ostia of arteries branching from the aorta (Figure 4B). In most animals, the plug surface was seen grossly to be completely covered by a new intima (in two animals the surface was only partially covered); the endothelial cell junctions were clearly outlined by silver and the cells contained sparse lipid (Figure 5). Epon sections showed that the new intimal layer covering the plug was continuous with the aortic intimal lining (Figure 6) and contained smooth muscle cells (Figure 7, A and B). Intracellular lipid droplets were present in the intimal thickening at the base of the plug and at the ostium between the aorta and renal artery.

Biophysical Models

Steady Flow

The hydrodynamic steady flow studies showed that very low shear stresses occurred upstream and downstream of the plug along the center line of the model aorta. High shear stresses up to 13 times baseline occurred on the surface 45° anterior and 30° posterior from the top of the plug. Very low fluid shear stresses were measured in a region surrounding the base of the plug, extending approximately 0.5 diameters upstream and downstream of the stenosis (Figure 8A). Along the wall opposite the plug, shear stresses reached 2–3 times baseline value (Figure 8B).

Although the mean flow was steady, fluctuating velocities were evident over part of the flow field. A horseshoe-shaped vortex began at the proximal base of the stenosis and curled along both sides (Figure 9A). One stagnation point, approximately 0.5 diameters upstream, was associated with a bound vortex. A second region of stagnation and recirculation extended for about 1 diameter downstream. The flow separated just beyond the top of the bulge. The inner stagnation/separation regions formed triangular shapes (Figure 9).

Unsteady Flow

In the unsteady flow studies, the pattern was similar to that of steady flow. The triangular region downstream of the stenosis was marked by low velocities and recirculation; a smaller, similar pattern was found upstream. The upstream region varied in size from 0.25 diameters at minimum flow to 0.5 diameters at peak flow, whereas the downstream region extended from 0.75 to 1.25 diameters.

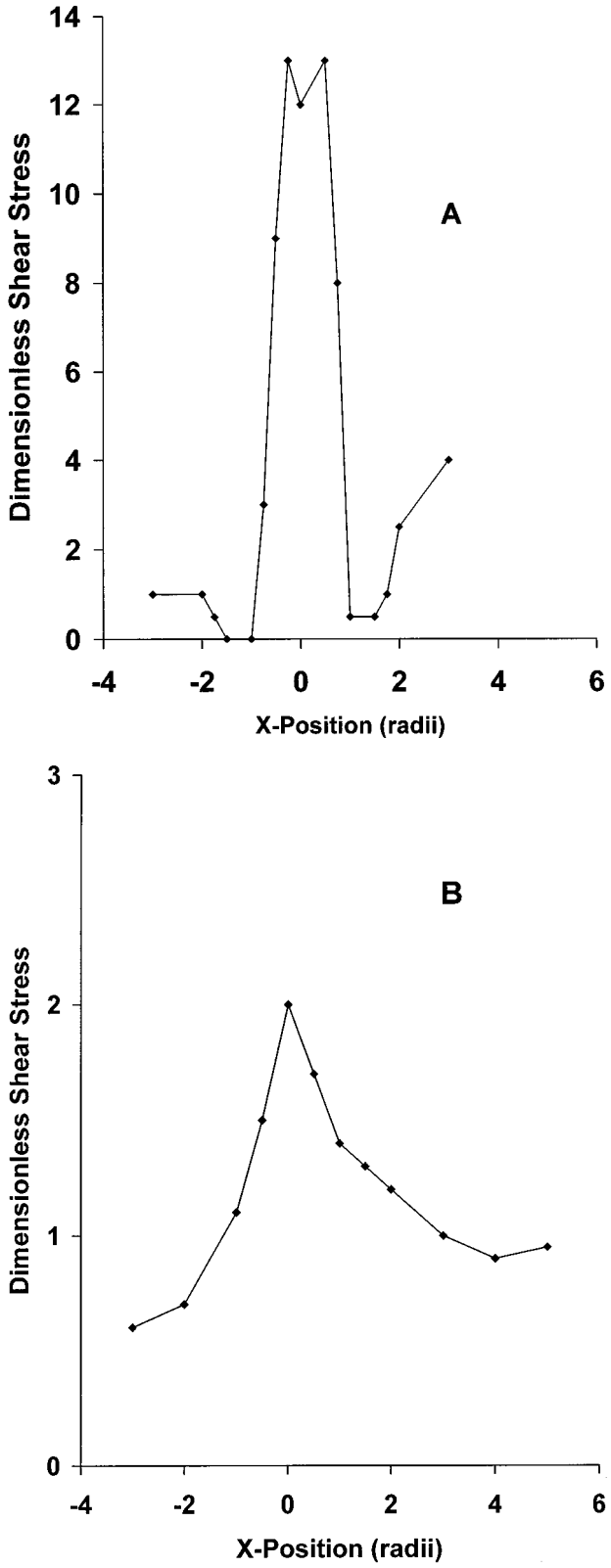

Figure 8. Normalized wall shear stress as a function of position, relative to the center of the hemispherical plug. The wall shear stress has been normalized using τ_o, the wall shear stress that would occur in the absence of the plug. A: Shear stress along the longitudinal centerline of the plug. B: Shear stress along the wall opposite the plug.

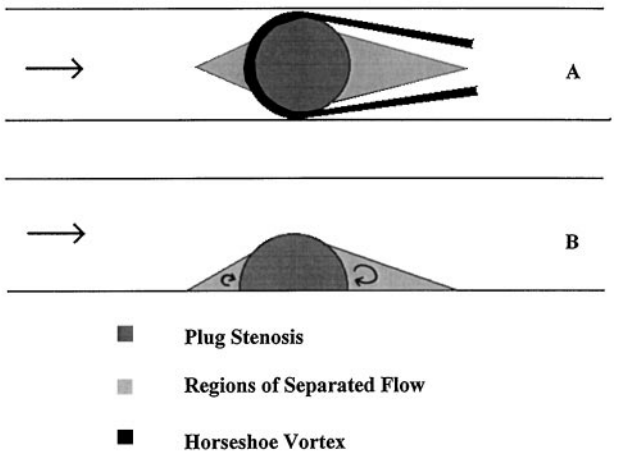

Figure 9. Regions of separated flow. These regions are characterized by recirculation and low shear. Results were obtained using dye injection in enlarged scale models. In unsteady flow, the proximal and distal dimensions of these regions oscillate with the frequency of the flow. The approximate location of the horseshoe vortex is shown in the top view. Flow is from left to right. A: Top view. B: Side view.

Due to the technique of plug insertion, the exact position and orientation of the plug within the aorta *in vivo* cannot be precisely determined. To determine the sensitivity of the flow field to the position of the plug, unsteady model studies were conducted with the plug tilted upstream at approximately 45° to the vessel axis. This increased the upstream stagnation region, which varied from 0.5 to 0.75 diameters, and the downstream region, which varied from 1 to 2 diameters. Within this downstream region a horseshoe vortex scoured the aortic wall with an aperiodic fluctuating velocity.

Discussion

The major objective of this work was to create an *in vivo* flow disturbance with well-defined regions of high and low fluid shear stress without causing significant alterations in intramural strains (defined as dimensionless measures of vessel deformation).[14] Both qualitative direct observations and quantitative studies in scaled physical models indicate that the plug stenosis achieves this objective. The regions of high and low shear stress are distinct. Elevated shear stresses occur on the wall opposite the plug; a similar finding was reported by Yamaguchi and Hanai,[30] who studied flow in a Plexiglas tube stenosed by a plug protruding into the lumen by one-eighth of the vessel diameter. Low shear stresses occur in crescent-shaped patches proximal and distal to the plug (Figures 8 and 9).

Tissue Response to the Plug

Locally, the aorta seemed to tolerate the plug well. The luminal surface was partly or completely overgrown by endothelium accompanied by a subendothelial layer of smooth muscle cells. This layer was thicker along the proximal and especially along the distal edge of the plug,

and therefore acquired a somewhat elongated shape (Figure 4B). This subendothelial thickening occurred in areas that were also subject to lipid deposition; it could therefore be a response to the lipid deposit, special local flow conditions (see discussion below), or both. Whatever its mechanism, this phenomenon suggests that raised atherosclerotic plaques should also tend to grow preferentially in the direction of flow.

Correlation of Biological and Biophysical Findings

In control rats (hypercholesterolemia without plug stenosis), the lipid deposits in the abdominal aorta were diffusely distributed with some accentuation around the ostia, as expected.[31] The effect of the plug was to alter the lipid distribution in a consistent manner. There were no lipid deposits in the intimal area opposite to the plug, whereas the base of the plug was surrounded by a heavy deposit of oil red O-positive lipid, advancing upstream 0.5 diameters on average and trailing downstream 1.5 diameters. The physical models of the plug stenosis indicate that the lipid-free area opposite the plug corresponds to increased fluid shear stress, whereas the regions proximal and distal to the base of the plug are areas of low shear stress, flow separation, and recirculation.

Fukushima and Azuma[32] conducted a detailed study of the steady flow field resulting from a hemispherical protuberance in a cylindrical vessel. They described a portion of the resulting flow field as a horseshoe vortex. As expected, the flow field in our models corresponds to their description. In unsteady flow, a horseshoe vortex was still observed but the extent of the separated regions varied over time. In models, the regions proximal and distal to the plug are characterized by flow separation, flow reversal, and low shear. These regions are strongly correlated with the crescent-shaped areas of lipid deposition *in vivo*. Similar findings have been inferred by others[31,33,34] studying the focal nature of atherosclerotic lesions. The plug stenosis further confirms these findings in a controlled *in vivo* experiment.

The sensitivity of the flow field to positioning of the plug within the rat aorta was investigated in model studies under conditions of unsteady flow. The general characteristics of the flow were unaltered even when the plug axis was tilted upstream at an angle of 45° rather than orthogonal to the flow. The size of the upstream and downstream separation regions increased as the plug axis was tilted; however, the flow field still contained a horseshoe vortex. These studies indicate that the *in vivo* flow field caused by the plug stenosis is relatively insensitive to experimental variations in plug deployment and renal branch angle.

In our prior studies of experimental aortic stenosis an external clip was used. The clip has a shielding effect that limits wall motion[14] in the throat of the stenosis. In such a system, fluid shear stress is very high beneath the clip, whereas the intramural stress and strain components are low. Under these conditions, the throat was spared from lipid deposition. These findings suggested that high fluid shear stress inhibited lipid deposition; however, as noted previously, the possible effect of low intramural stress could not be completely discounted. The hemispherical plug stenosis demonstrates that in the presence of normal intramural strains, increased shear correlates with decreased lipid deposition. Thus, the present study adds strong evidence to support the contention that increased shear inhibits lipid deposition. Our studies do not address the mechanism whereby low shear stress favors lipid deposition; extensive work is being performed in this area, focusing especially on endothelial mechanotransduction[35,36] and flow-mediated regulation of endothelial gene expression.[37–39]

Finally, the ring of intima in contact with the base of the plug is also an area of lipid deposition. However, the intima in very close proximity to the base of the plug is likely to experience altered stresses and strains. Hence, this ring of lipid deposition cannot be directly and exclusively attributed to disturbed flow.

In summary, the hemispherical plug stenosis minimizes the potentially confounding effects of intramural parameters on the data related to shear stresses. *In vivo* studies using the plug stenosis can focus more sharply on the relationship between lipid deposition and hydrodynamic disturbances. Our results show that elevated shear stress reduces lipid deposition, whereas low shear and recirculation promote lipid deposition.

Acknowledgments

The following WPI students assisted in the physical modeling studies: Brian Abraham, Christine Calvert, Annemarie Currier, Jeffrey Duquette, Hedi Franklin, Donald Peterson, Charles Stankewicz, and Stephen Williams. We thank Kathleen Wortham and L. Zhang for help with the microsurgery.

References

1. Giddins DP, Zarins CK, Glagov S: The role of fluid mechanics in the localization and detection of atherosclerosis. J Biomech Eng 1993, 115:588–594
2. Nerem RM: Vascular fluid mechanics, the arterial wall, and atherosclerosis. J Biomech Eng 1992, 114:274–282
3. Lei M, Kleinstrever C, Truskey GA: Numerical investigation and prediction of atherogenic sites in branching arteries. J Biomech Eng 1995, 117:350–357
4. Fry DL: Acute vascular endothelial changes associated with increased blood velocity gradients. Circ Res 1968, 22:165–197
5. Glagov S, Ts'ao C: Restitution of aortic wall after sustained necrotizing transmural ligation injury. Am J Pathol 1975, 79:7–30
6. Gerrity RG, Naito HK: Alteration of endothelial cell surface morphology after experimental aortic coarctation. Artery 1980, 8:267–274
7. Reidy MA, Langille BL: The effect of local blood flow patterns on endothelial cell morphology. Exp Mol Pathol 1980, 32:276–289
8. Greenhill NS, Stehbens WE: Scanning electron microscopic study of the anastomosed vein of arteriovenous fistulae. Atherosclerosis 1981, 39:383–393
9. Joris I, Zand T, Majno G: Hydrodynamic injury of the endothelium in acute aortic stenosis. Am J Pathol 1982, 106:394–408
10. Legg MJ, Gow BS: Scanning electron microscopy of endothelium around an experimental stenosis in the rabbit aorta using a new casting material. Atherosclerosis 1982, 42:299–318

11. Langille BL, Reidy MA, Kline RL: Injury and repair of endothelium at sites of flow disturbances near abdominal aortic coarctations in rabbits. Arteriosclerosis 1986, 6:146–154
12. Levesque MJ, Liepsch D, Moravec S, Nerem RM: Correlation of endothelial cell shape and wall shear stress in a stenosed dog aorta. Arteriosclerosis 1986, 6:220–229
13. Zand T, Nunnari JJ, Hoffman AH, MacWilliams B, Majno G, Joris I: Endothelial adaptations in aortic stenosis: correlation with flow parameters. Am J Pathol 1988, 133:407–418
14. Zand T, Majno G, Nunnari JJ, Hoffman AH, Savilonis BJ, MacWilliams B, Joris I: Lipid deposition and intimal stress and strain: a study in rats with aortic stenosis. Am J Pathol 1991, 139:101–113
15. Dewey CF Jr, Bussolari SR, Gimbrone MA Jr, Davies PF: The dynamic response of vascular endothelial cells to fluid shear stress. J Biomech Eng 1981, 103:177–185
16. White GE, Fujiwara K, Shefton EJ, Dewey CF, Gimbrone MA Jr.: Fluid shear stress influences cell shape and cytoskeleton organization in cultured vascular endothelium. Fed Proc 1982, 41:321
17. Franke R-P, Gräfe M, Schnittler H, Seiffge D, Mittermayer C, Drenckhahn D: Induction of human vascular endothelial stress fibers by fluid shear stress. Nature 1982, 307:648–649
18. Eskin SG, Ives CL, McIntire LV, Navarro LT: Response of cultured endothelial cells to steady flow. Microvasc Res 1984, 28:87–94
19. Nerem RM, Sato M, Levesque MJ: Elongation orientation and effective shear modulus of cultured endothelial cells in response to shear. Fed Proc 1985, 44:1659
20. Levesque MJ, Nerem RM: The elongation and orientation of cultured endothelial cells in response to shear stress. J Biochem Eng 1985, 107:341–347
21. Wechezak AR, Viggers RF, Sauvage LR: Fibronectin and F-actin redistribution in cultured endothelial cells exposed to shear stress. Lab Invest 1985, 53:639–647
22. Ives CL, Eskin SG, McIntire LV: Mechanical effects on endothelial cell morphology: in vitro assessment. In Vitro Cell Dev Biol 1986, 22:500–507
23. Viggers RF, Wechezak AR, Sauvage LR: An apparatus to study the response of cultured endothelium to shear stress. J Biochem Eng 1986, 108:332–337
24. Chiu JJ, Wang DL, Chien S, Skalak R, Usami S: Effects of disturbed flow on endothelial cells. J Biomech Eng 1998, 120:2–8
25. Friedman MH: Arteriosclerosis research using vascular flow models: from 2-D branches to compliant replicas. J Biomech Eng 1993, 115:595–601
26. Buchanan JR Jr, Kleinstreuer C: Simulation of particle-hemodynamics in a partially occluded artery segment with implications to the initiation of microemboli and secondary stenoses. J Biomech Eng 1998, 120:446–454
27. Lyon RT, Runyon-Hass A, Davis HR, Glagov S, Zarins CK: Protection from atherosclerosic lesion formation by reduction of artery wall motion. J Vasc Surg 1987, 5:59–67
28. Joris I, Zand T Nunnari JJ, Krolikowski FJ, Majno G: Studies on the pathogenesis of atherosclerosis. I. Adhesion and emigration of mononuclear cells in the aorta of hypercholesterolemic rats. Am J Pathol 1983, 113:341–358
29. Fung YC: Biomechanics Circulation. 2nd ed, New York, Springer, 1997, pp 48, 131–132
30. Yamaguchi T, Hanai S: To what extent does a minimal atherosclerotic plaque alter the arterial wall shear stress distribution? A model study by an electrochemical method. Biorheology 1988, 25:31–36
31. Okano M, Yoshido Y: Endothelial cell morphometry of atherosclerotic lesions and flow profiles at aortic bifurcations in cholesterol fed rabbits. J Biomech Eng 1992, 114:301–308
32. Fukushima T, Azuma T: The horseshoe vortex: a secondary flow generated in arteries with stenosis, bifurcation, and branchings. Biorheology 1982, 19:143–154
33. Caro CG, Fitz-Gerald JM, Schroter RC: Arterial wall shear and distribution of early atheroma in man. Nature 1969, 223:1159–1161
34. Ku DN, Giddens DP, Zarins CK, Glagov S: Pulsatile flow and atherosclerosis in the human carotid bifurcation: positive correlations between plaque location and low and oscillating shear stress. Arteriosclerosis 1985, 5:293–302
35. Malek AM, Izumo S: Molecular aspects of signal transduction of shear stress in the endothelial cell. J Hypertension 1994, 12:989–999
36. Davies PF: Flow-mediated endothelial mechanotransduction. Physiol Rev 1995, 75:519–560
37. Malek AM, Izumo S: Control of endothelial cell gene expression by flow. J Biomech 1995, 28:1515–1528
38. Resnick N, Gimbrone MA, Jr: Hemodynamic forces are complex regulators of endothelial gene expression. FASEB J 1995, 9:874–882
39. Ando J, Kamiya A: Flow-dependent regulation of gene expression in vascular endothelial cells. Jpn Heart J 1996, 37:19–32